Photoluminescence enhancement induced from silver nanoparticles in Tb^{3+}-doped glass ceramics

Gang Bi (毕 岗)[1], Li Wang (王 丽)[2], Wei Xiong (熊 巍)[1], Kosi Ueno[3,4], Hiroaki Misawa[3], and Jianrong Qiu (邱建荣)[2*]

[1]*School of Information and Electrical, Zhejiang University City College, Hangzhou 310015, China*

[2]*State Key Laboratory of Silicon Materials, Zhejiang University, Hangzhou 310027, China*

[3]*Research Institute for Electronic Science, Hokkaido University, Sapporo 001-0021, Japan*

[4]*PRESTO, Japan Science and Technology Agency, Kawaguchi 332-0012, Japan*

[*]*Corresponding author: qjr@zju.edu.cn*

Received February 5, 2012; accepted March 28, 2012; posted online July 13, 2012

We experimentally verify that surface plasmon (SP) enhances the photoluminescence (PL) of visible light from Tb^{3+}-doped $60SiO_2$-$20Al_2O_3$-$20CaF_2$:$0.3Tb^{3+}$, $20Yb^{3+}$ glass ceramics by using electron beam lithography to fabricate silver nanoparticles on the surface of the glass ceramics. Numerical calculation for the SP enhancement spectroscopy is achieved by using the finite-difference time-domain algorithm. A PL enhancement of Tb^{3+} by as much as 1.6 times is observed. The PL enhancement is mainly due to the coupling of excitation from $^7F_6$ to $^5D_4$ transition dipole of Tb^{3+} ion with SP mode induced from the silver nanoparticles.

OCIS codes: 240.6680, 240.6695, 240.4350, 310.6188.
doi: 10.3788/COL201210.092401.

Photoluminescence (PL) effects enhanced by the surface plasmon (SP) of noble metal nanostructures on different materials[1] have attracted much attention for their scientific significance and application potentials in biosensor[2], molecular electronics[3], and solid-state lighting[4,5]. For instance, Neal *et al.*[4,6] observed multifold enhancement of visible-light emission from dye-doped polymers with the use of SP coupling in unpatterned silver film. However, previous works were mostly focused on the PL materials of dye-doped polymers. Few works have focused on the PL materials of rare-earth-ion-doped inorganic materials. Moreover, the PL materials used were mostly two-dimensional (2D) films, and bulk materials had rarely been investigated. Some studies on the enhancement of luminescence from glass co-doped with rare earth ions and noble metal nanoparticles (NPs) have been reported[7−9]. However, modifying the SP resonance (SPR) frequency is difficult because controlling the size and alignment of the noble NPs in the glass matrix through heat treatment is likewise difficult. Mertens *et al.* observed an enhancement of the PL intensity at 1.54 μm of optically active Er^{3+} ions in SiO_2 by coupling them to engineered silver NPs[5]. The silver NPs were fabricated using electron beam lithography (EBL), Ag evaporation, and lift-off. The sample used was Er-doped SiO_2 substrate. The Er ions were in the top 50 nm of SiO_2 substrates, which were considered as 2D materials, not bulk material.

We achieved the SP-assisted enhancement of PL in bulk glass ceramics doped with rare earth ions, and fabricated silver nanorods on the glass ceramics by EBL and lift-off technique[10]. The huge advantages of EBL and lift-off technique above other common fabrication schemes for metal NPs (chemical production or thermally vacuum deposited metal island films) are its unsurpassed design flexibility and particle monodispersity and homogeneity. To our knowledge, this study is the first to report an observation of enhanced PL from glass ceramics by SP-assisted silver NPs fabricated by EBL and lift-off technique. In this letter, we choose a glass ceramic of $60SiO_2$-$20Al_2O_3$-$20CaF_2$:$0.3Tb^{3+}$ -$20Yb^{3+}$ (mol%) composition as the substrate because it is a good substrate for fabricating silver NPs on its surface using EBL and lift-off technique and because it shows excellent luminescence property[11]. Reagent-grade (4N-grade) powders were mixed together and melted in a corundum crucible for 30 min at 1 400 °C under ambient atmosphere. Then, the melt was poured into a stainless plate and pressed to a thickness of approximately 2 mm by another plate. The melt was then quenched to room temperature. After the glass samples were cut and polished, a transparent and colorless glass sample of good optical quality was obtained. Differential thermal analysis measurements were carried out in the differential thermal analyzer (SDT Q600), from which we determined a thermal treatment temperature of 675 °C for 5 h to obtain transparent glass ceramic containing CaF_2:Tb^{3+} ,Yb^{3+} NPs[11]. The glass ceramic samples were then cut and polished. For plasmonic field enhancement, a 30×30 (μm) area of silver nanorod measuring 100×100×60 (nm) was fabricated on the Tb^{3+}-doped glass ceramic substrates surface by high-resolution EBL on a scanning electron microscope (SEM, ELS-7 700) at a 100-kV accelerating voltage and lift-off of a silver monolayer deposited by sputtering. The precision of the positioning and dimensions of the nanorods was better than 2 nm; hence, identical nanorods were patterned. The structures were spaced 120 nm from one another, as shown in Fig. 1.

Silver was chosen because this metal exhibited the lowest Ohmic damping at visible and infrared (IR) frequencies, thereby giving rise to the highest electromagnetic field enhancements[12].

The measurement of optical extinction spectra was introduced as follows. For transmission measurements in

the visible and near IR region (400–950 nm), a halogen light beam was passed through a pinhole (diameter of 200 μm) and introduced into an optical microscope (Optiphot 2), where it was focused on the sample by a microscope objective (20×, NA=0.4). By focusing a quasi-parallel probe beam, a waist of approximately 8 μm was attained at the focus. The transmitted beam was collected by a multi-channel photodetector (PMA-11), which recorded its spectrum normalized to the spectrum of the incident beam. The PL spectra were measured by the Ar-ion laser at 488 nm and confocal microscope with the lens of 40× (NA=0.5). Figure 2 shows PL spectra of Tb^{3+} ions doped in glass ceramics. The excitation wavelength was 488 nm. The solid line indicates the PL spectrum obtained from areas without silver nanorods, whereas the dotted line indicates the PL spectrum obtained from areas with silver nanorods. With excitation at 488 nm, emission of Tb^{3+} ions occurred at 537, 578, and 612 nm, which can be assigned to the transitions from $^5D_4$ to $^7F_5$, $^7F_4$, and $^7F_3$ levels, respectively. Compared with the PL intensity from the area without silver nanorods, the PL intensity from the area with silver nanorods was stronger. The enhancement factors were 1.60, 1.56, and 1.59 for different PL intensity peaks of Tb^{3+} ions at 537, 578, and 612 nm, respectively.

Finite-difference time-domain (FDTD) simulation modeling of linear Maxwell's equations (Lumerical FDTD Solution 7.0) was adopted to calculate the extinction spectrum and enhancement of electrical field intensity[13].

We tested the luminescence measurement at different positions of the area covered with silver nanorods. Compared with the area without silver nanorods, the average PL enhancement factor was approximately 1.6.

In order to identify the mechanism of the PL enhancement of Tb^{3+} ions, we measured the optical extinction spectrum of the silver nanorod structures (Fig. 3). The green dashed and blue dotted lines exhibit the excitation and emission spectra of Tb^{3+} ions in this glass ceramic, respectively. The optical extinction spectrum shows a single peak near 485 nm, covering the excitation and emission bands of Tb^{3+} ions in this glass ceramic.

The red dash-dot line shows the calculated extinction spectrum of the silver nanorods. We can see that the experimental extinction spectrum nearly matches the calculated one. That is why we chose the geometry of silver nanorods of 100×100×60 (nm). The extinction spectra can be tuned by changing the geometry of silver nanorods.

Because the extinction spectrum of silver nanorods covered the excitation and emission bands of Tb^{3+} ions, we supposed that the observed PL enhancement was due

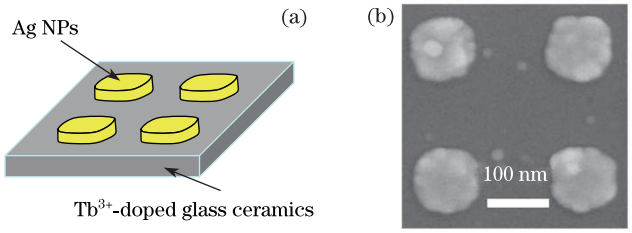

Fig. 1. (a) Schematic of Ag NPs on glass ceramic surface and (b) SEM image of silver nanorods.

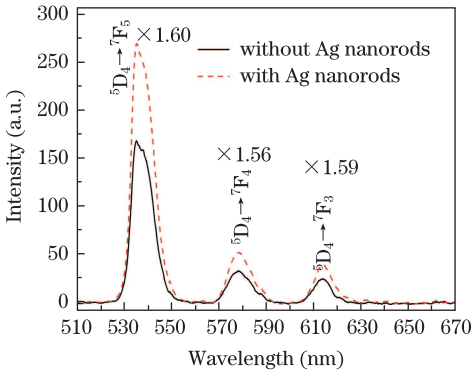

Fig. 2. (Color online) PL spectra of Tb^{3+} ions doped in glass ceramics: no silver nanorods on glass ceramic surface (black); with silver nanorods on glass ceramic surface (red). Excitation wavelength is 488 nm.

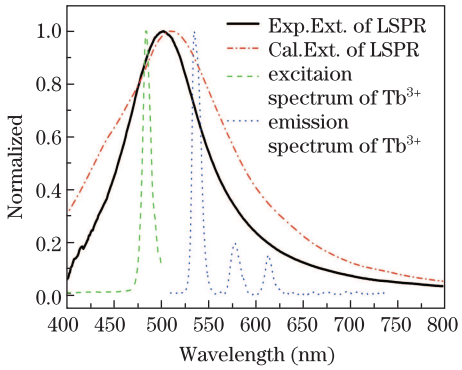

Fig. 3. (Color online) Extinction spectra of silver nanorods array pattern and excitation spectrum of Tb^{3+} ions. LSPR: localized SPR.

to the coupling of excitation of the $^7F_6$ to $^5D_4$ transition dipole and the emissions of $^5D_4$ to $^7F_5$, $^5D_4$ to $^7F_4$, and $^5D_4$ to $^7F_3$ transitions of Tb^{3+} ions with SP mode induced from the silver nanorods.

The silver nanorod can, in some sense, be seen as a resonator for SP. Thus, similarly to any (moderately damped) resonator, if excited resonantly, the oscillation amplitude can overcome the excitation amplitude by several orders of magnitude. For SP on the silver nanorods, this technique results in a strong enhancement of the local electric field compared to the exciting electric field. Hence, we also made the qualitative theoretical confirmation of this claim, which was possible from the spatial profiles of the optical near field.

Figure 4 shows the electric field intensity enhancement factor mapping (with respect to the incident intensity) at the wavelengths of 486 nm (close to excitation wavelength of Tb^{3+} ion) and 540, 582, and 612 nm (close to emission wavelength of Tb^{3+} ion) for the silver nanostructures. The maximum electrical field intensity at 486 nm was approximately 136 times. At the wavelengths of 540, 582, and 612 nm, which are close to the $^5D_4$ to $^7F_5$, $^5D_4$ to $^7F_4$, and $^5D_4$ to $^7F_3$ transitions of Tb^{3+}, the maximum electric field enhancement factors are approximately 69, 63, and 44 times, which are smaller than the maximum enhancement factor at 486 nm.

For the maximum electric field enhancement factor of emission wavelengths 540, 582, and 612 nm of Tb^{3+} ion,

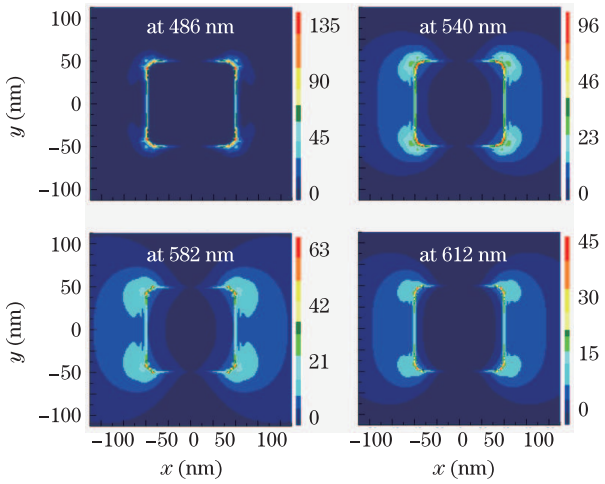

Fig. 4. (Color online) Calculated electric field enhancement factor mapping at the wavelengths of 486, 540, 582, and 612 nm.

the largest enhancement factor is 69 at 540 nm, which is 1.1 times as large as the one at 582 nm and 1.6 times as large as the one at 612 nm. However, the PL enhancement factor at 537 nm was the same as the one at 578 and 612 nm.

Because the relationship of electric field enhancement factor of the three emission wavelengths of Tb^{3+} ion and the relationship of PL enhancement factor of three emission wavelengths of Tb^{3+} ion were different, and because the electrical field intensity enhancement factor at excitation wavelength of Tb^{3+} ion was twice as large as that at its emission wavelengths, we believed that the PL enhancement was mainly due to the coupling of excitation of the $^7F_6$ to $^5D_4$ transition dipole of Tb^{3+} ion.

In conclusion, we achieve ∼1.6-times enhancement of the PL intensity peaks at 537, 578, and 612 nm of Tb^{3+} ions doped in $60SiO_2$-$20Al_2O_3$-$20CaF_2$:$0.3Tb^{3+}$, $20Yb^{3+}$ glass ceramic by coupling them to engineered silver nanorods. The PL enhancement is maximal if the excitation of Tb^{3+} emission is resonant with silver nanorod SP modes. The electric field enhancement factor is calculated by FDTD simulation. Both these observations demonstrate that the PL enhancement is mainly due to $^7F_6$ to $^5D_4$ transition dipoles of Tb^{3+}coupling with silver nanorod SP modes.

This work was supported by the National Natural Science Foundation of China (Nos. 50672087, 50872123, and 50802083) and the Natural Science Foundation of Zhejiang province in China (No. Y1110499). H. Misawa also acknowledges funding from the Ministry of Education, Culture, Sports, Science, and Technology of Japan; KAKENHI Grants-in-Aid (No. 19049001); a Grant-in-Aid from Hokkaido Innovation through Nano Technology Support.

References

1. H. Raether, *Surface Plasmons on Smooth and Rough Surfaces and on Gratings* (Springer, Toronto, 1988).
2. P. P. Pompa, L. Martiradonna, A. D. Torre, F. D. Sala, L. Manna, M. De Vittorio, F. Calabi, R. Cingolani, and R. Rinaldi, Nat. Nanotechnol. **1,** 126 (2006).
3. J. Zhang, Y. Fu, M. H. Chowdhury, and J. R. Lakowicz, Nano Lett. **7,** 2101 (2007).
4. T. D. Neal, K. Okamoto, and A. Scherer, Opt. Express **13,** 5522 (2005).
5. H. Mertens and A. Polman, Appl. Phys. Lett. **89,** 211107 (2006).
6. P. Cheng, D. Li, Z. Yuan, P. Chen, and D. Yang, Appl. Phys. Lett. **92,** 041119 (2008).
7. T. Som and B. Karmakar, J. Appl. Phys. **105,** 013102 (2009).
8. L. R. P. Kassab, R. de Almeida, D. M. da Silva, and C. B. de Araújo, J. Appl. Phys. **104,** 093531 (2008).
9. V. K. Rai, L. de S. Menezes, C. B. de Araújo, L. R. P. Kassab, D. M. da Silva, and R. A. Kobayashi, J. Appl. Phys. **103,** 093526 (2008).
10. K. Ueno, S. Juodkazis, V. Mizeikis, K. Sasaki, and H. Misawa, Opt. Lett. **30,** 2158 (2005).
11. S. Ye, B. Zhu, J. Chen, J. Luo, and J. Qiu, Appl. Phys. Lett. **92,** 141112 (2008).
12. U. Kreibig and M. Vollmer, *Optical Properties of Metal Clusters* (Springer, Berlin, 1995) Chap. 2.
13. L. Wang, W. Xiong, Y. Nishijima, Y. Yokota, K. Ueno, H. Misawa, J. Qiu, and G. Bi, Appl. Opt. **50,** 5600 (2011).